THE JOURNAL OF BIOLOGICAL CHEMISTRY
Vol. 279, No. 17, Issue of April 23, pp. 16947–16953, 2004

Printed in U.S.A.

Characterization and Metabolic Function of a Peroxisomal Sarcosine and Pipecolate Oxidase from *Arabidopsis**

Received for publication, January 5, 2004, and in revised form, February 6, 2004
Published, JBC Papers in Press, February 6, 2004, DOI 10.1074/jbc.M400071200

Aymeric Goyer‡, Tanya L. Johnson§, Laura J. Olsen§, Eva Collakova¶, Yair Shachar-Hill¶, David Rhodes‖, and Andrew D. Hanson‡**

From the ‡Horticultural Sciences Department, University of Florida, Gainesville, Florida 32611, the §Department of Molecular, Cellular, and Developmental Biology, University of Michigan, Ann Arbor, Michigan 48109, the ¶Department of Plant Biology, Michigan State University, East Lansing, Michigan 48824, and the ‖Department of Horticulture, Purdue University, West Lafayette, Indiana 47907

Sarcosine oxidase (SOX) is known as a peroxisomal enzyme in mammals and as a sarcosine-inducible enzyme in soil bacteria. Its presence in plants was unsuspected until the *Arabidopsis* genome was found to encode a protein (AtSOX) with ~33% sequence identity to mammalian and bacterial SOXs. When overexpressed in *Escherichia coli*, AtSOX enhanced growth on sarcosine as sole nitrogen source, showing that it has SOX activity *in vivo*, and the recombinant protein catalyzed the oxidation of sarcosine to glycine, formaldehyde, and H_2O_2 *in vitro*. AtSOX also attacked other *N*-methyl amino acids and, like mammalian SOXs, catalyzed the oxidation of L-pipecolate to Δ^1-piperideine-6-carboxylate. Like bacterial monomeric SOXs, AtSOX was active as a monomer, contained FAD covalently bound to a cysteine residue near the C terminus, and was not stimulated by tetrahydrofolate. Although AtSOX lacks a typical peroxisome-targeting signal, *in vitro* assays established that it is imported into peroxisomes. Quantitation of mRNA showed that AtSOX is expressed at a low level throughout the plant and is not sarcosine-inducible. Consistent with a low level of AtSOX expression, *Arabidopsis* plantlets slowly metabolized supplied [^{14}C]sarcosine to glycine and serine. Gas chromatography-mass spectrometry analysis revealed low levels of pipecolate but almost no sarcosine in wild type *Arabidopsis* and showed that pipecolate but not sarcosine accumulated 6-fold when AtSOX expression was suppressed by RNA interference. Moreover, the pipecolate catabolite α-aminoadipate decreased 30-fold in RNA interference plants. These data indicate that pipecolate is the endogenous substrate for SOX in plants and that plants can utilize exogenous sarcosine opportunistically, sarcosine being a common soil metabolite.

Sarcosine (*N*-methylglycine) is a key metabolite of the mammalian liver, where it is formed from glycine by the action of glycine *N*-methyltransferase or from the oxidation of glycine betaine (1, 2). Sarcosine is also a common soil metabolite of creatinine, which animals excrete in urine, and various soil bacteria can utilize sarcosine as a nitrogen and carbon source (3, 4). Mammals and certain soil bacteria share the capacity to oxidatively demethylate sarcosine, yielding formaldehyde, glycine, and H_2O_2 (4, 5). This reaction is mediated by sarcosine oxidase (SOX, EC 1.5.3.1).[1] SOXs are constitutive enzymes in mammals (5, 6) but are induced by sarcosine in bacteria (3).

Bacterial and mammalian SOXs belong to a recently recognized family of enzymes that catalyze oxidative reactions with secondary or tertiary amino acids and contain covalently bound flavin (5, 7). The archetypal family members are the monomeric SOXs (MSOXs) of bacteria such as *Bacillus* sp. MSOXs are active as monomers, have a molecular mass of ~44 kDa, an N-terminal ADP-binding motif, and contain FAD bound to a conserved cysteine residue (7, 8). *Bacillus* MSOX also acts on *N*-methyl-L-alanine, *N*-ethylglycine, and L-proline (9). Mammalian SOXs are closely related to MSOXs and are alternatively named pipecolate oxidases (PIPOXs) because L-pipecolate is also a good substrate (5). Mammalian SOX/PIPOXs have C-terminal tripeptide peroxisomal targeting signal 1 (PTS1) motifs and are located in peroxisomes (5, 6). Other members of the MSOX family include *Escherichia coli N*-methyltryptophan oxidase (8), the NikD enzyme of *Streptomyces tendae* (10), and *Bacillus subtilis* glycine oxidase (11). More distant family members are heterotetrameric bacterial SOXs, and mammalian sarcosine and dimethylglycine dehydrogenases (7).

There seems to be little evidence that sarcosine is a natural plant product (12) and none at all that plants have pathways leading to sarcosine from glycine, glycine betaine, or creatinine (13, 14). It was therefore initially surprising to find that *Arabidopsis* has a gene (*At2g24580*) encoding a close homolog of bacterial MSOXs and mammalian SOX/PIPOXs and that other plants have similar genes (15, 16). However, consistent with there being sarcosine-oxidizing activity in plants, sarcosine application induced expression of formate dehydrogenase in potato leaves (17). As this enzyme is induced in plants by formaldehyde or formate (17–19), its induction by sarcosine could be explained by the release of formaldehyde. Moreover, pipecolate is a catabolite of lysine in plants (20) and occurs

* This work was supported in part by the Florida Agricultural Experimental Station, by an endowment from the C. V. Griffin, Sr. Foundation, and by Grants MCB-0114117 and MCB-0327241 from the National Science Foundation and approved for publication as Journal Series number R.09954. The costs of publication of this article were defrayed in part by the payment of page charges. This article must therefore be hereby marked "*advertisement*" in accordance with 18 U.S.C. Section 1734 solely to indicate this fact.

** To whom correspondence should be addressed: Horticultural Sciences Dept., University of Florida, P. O. Box 110690, Gainesville, Florida 32611. Tel.: 352-392-1928 (ext. 334); Fax: 352-392-5653; E-mail: adha@mail.ifas.ufl.edu.

[1] The abbreviations used are: SOX, sarcosine oxidase; EST, expressed sequence tag; GC-MS, gas chromatography-mass spectrometry; MALDI-TOFMS, matrix-assisted laser desorption ionization time-of-flight mass spectrometry; MSOX, monomeric SOX; P2C, Δ^1-piperideine-2-carboxylate; P6C, Δ^1-piperideine-6-carboxylate; PIPOX, pipecolate oxidase; PTS, peroxisomal targeting signal; RNAi, RNA interference; RT-PCR, reverse transcription PCR; Mes, 4-morpholineethanesulfonic acid

widely (12) so that, like mammals, plants might be expected to have PIPOX activity.

To assign a function to the *Arabidopsis* SOX homolog, we first used a functional assay in *E. coli* to demonstrate that it has SOX activity *in vivo* and showed that the recombinant protein has SOX and PIPOX activity. We then characterized the enzyme further, showed that it is imported into peroxisomes, and confirmed that *Arabidopsis* can oxidize sarcosine *in vivo*. Lastly, we analyzed levels of sarcosine and pipecolate in plants with suppressed SOX expression and wild type controls.

EXPERIMENTAL PROCEDURES

Chemicals and Reagents—[*N*-methyl-^{14}C]Sarcosine (55 mCi/mmol) and [carboxyl-^{14}C]sarcosine (50 mCi/mmol) were obtained from American Radiolabeled Chemicals (St. Louis, MO), [^{14}C]formaldehyde (54 mCi/mmol) was from PerkinElmer Life Sciences, and Redivue™ [^{35}S]methionine (1180 Ci/mmol) was from Amersham Biosciences. Specific radioactivities were adjusted as needed with unlabeled compound. (6*R*,6*S*)-Tetrahydrofolate was from Schircks Laboratories (Jona, Switzerland). Other biochemicals were from Sigma. Ion exchange resins were from Bio-Rad. PeroXOquant peroxide assay kits were from Pierce. Cellulose TLC plates (0.1-mm layer thickness) were from Merck.

Plants and Growth Conditions—Arabidopsis thaliana (ecotype Columbia) plants were grown at 23 °C in 12-h days (photosynthetic photon flux density of 80 microeinstein m^{-2} s^{-1}) in potting soil irrigated with water; and when roots were required, plants were grown in hydroponic culture as described (21). Pumpkin seeds (*Cucurbita pepo*, cv. Connecticut Fields) were purchased from Siegers Seed Co. (Zeeland, MI). Pumpkin seedlings were grown in moist vermiculite for 6 days in the dark at 25–28 °C.

cDNA Isolation and Expression in E. coli—Expressed sequence tag (EST) GenBank™ accession number T41826 encoding AtSOX was obtained from the *Arabidopsis* Biological Resource Center (Columbus, OH), sequenced, and cloned into pET-43.1a (Novagen) as follows. *Pfu* DNA polymerase (Stratagene) was used to amplify the cDNA using the primers 5′-ATATACATATGGAATATTCCGAC-3′ (forward) and 5′-TATATCTCGAGTTAATGTTTCAATGG-3′ (reverse). The resulting amplicon was digested with NdeI and XhoI and cloned between the same sites of pET-43.1a. This construct (pET43-SOX) was electroporated into *E. coli* DH10B cells, verified by sequencing, and electroporated into *E. coli* Rosetta™ (DE3) cells (Novagen). For enzyme production, cells were grown at 37 °C in LB medium containing 100 μg/ml ampicillin and 34 μg/ml chloramphenicol until A_{600} reached 0.6. Isopropyl-D-thiogalactopyranoside was then added (final concentration 100 μM), and incubation continued for 18 h at 25 °C.

RNA Interference (RNAi) Experiments—A 475-bp AtSOX cDNA fragment was amplified using the primers 5′-CACCATTCGACGTGATTGTCGT-3′ (forward) and 5′-TCCAATCGCAAGCGTCTG-3′ (reverse), and the amplicon was cloned into the pENTR/D-TOPO® vector using the pENTR™ Directional TOPO® Cloning Kit (Invitrogen) according to the manufacturer's instructions. The SOX sequence was then transferred into the pHELLSGATE8 vector (22) using the LR Clonase™ recombination method (Invitrogen). The sequence-verified pHELLSGATE-SOX construct was introduced into *Agrobacterium tumefaciens* strain ABI. *Arabidopsis* plants (ecotype Columbia) were transformed by the vacuum infiltration method (23). Kanamycin-resistant T2 plants were used for real time quantitative RT-PCR analyses and amino acid analyses.

Utilization of Sarcosine as Nitrogen Source by E. coli Overexpressing AtSOX—Cells were plated on M9 minimal medium (24) minus NH_4Cl, containing trace elements (25), 0.4% glucose, 1.5% agar, 100 μg/ml ampicillin, 34 μg/ml chloramphenicol, 100 μM isopropyl-D-thiogalactopyranoside, and 17.5 mM sarcosine or 2.2 mM glycine as the nitrogen source (filter-sterilized, added after autoclaving). Growth was at 25 °C.

Enzyme Assays—Oxidase assays were carried out at 30 °C in 50 mM Tris-HCl, pH 8.0, in 20-μl reaction mixtures in 1.5-ml microcentrifuge tubes. Product formation was linear with time and enzyme level. Tests with various assay volumes and with O_2 instead of air as headspace gas indicated that O_2 diffusion did not significantly limit the reaction rate. For routine assays, substrates were unlabeled, H_2O_2 formation was estimated colorimetrically with the PeroXOquant kit, and incubation time was 60 min. K_m and k_c values were estimated by curve-fitting to the Michaelis-Menten equation using non-linear regression; the enzyme was taken to be 90% pure. K_m and k_c data are the means of three determinations, and S.E. values were <5% of the means. To determine stoichiometry, formaldehyde and glycine formation were quantified radiochemically, respectively using [*N*-methyl-^{14}C]sarcosine or [carboxyl-^{14}C]sarcosine (55 nCi/assay, plus unlabeled sarcosine to give a total concentration of 10 mM). The [^{14}C]formaldehyde assay was also used during protein purification. To determine [^{14}C]formaldehyde, a 10-μl portion of the reaction mixture was stopped by adding 75 μl of 1 M sodium acetate, pH 4.5, 5 μl of 1 M formaldehyde, and 75 μl of 400 mM dimedone in 50% ethanol and boiled for 5 min. The ^{14}C product was extracted into 1 ml of toluene, and an 0.8-ml aliquot was taken for scintillation counting. Data were corrected for recovery of [^{14}C]formaldehyde spikes. To determine [^{14}C]glycine, an aliquot of the reaction mixture was mixed with an equal volume of acetone to stop the reaction, and subjected to thin layer electrophoresis at 4 °C for 20 min at 1.8 kV in 1.5 M formic acid. [^{14}C]Glycine zones were located by autoradiography, scraped from the plate, and quantified by scintillation counting. Data were corrected for recovery.

Protein Purification and Molecular Mass Determination—Operations were at 0–4 °C. Rosetta™ cells from a 1-liter culture were harvested by centrifugation, resuspended in 11 ml of 50 mM Tris-HCl, pH 8.0 (buffer A), and broken in a Mini-BeadBeater (Biospec Products, Bartlesville, OK) using 0.1-mm zirconia/silica beads. After centrifugation (20,000 × *g*, 30 min), the supernatant was subjected to 30–50% (w/v) $(NH_4)_2SO_4$ fractionation; after centrifugation (20,000 × *g*, 30 min) the pellet was dissolved in 2.6 ml of buffer A and desalted on two in-series PD-10 columns (Amersham Biosciences) equilibrated in buffer A. Subsequent steps used a Waters 626 high pressure liquid chromatography system. Proteins were loaded on a MonoQ HR 5/5 column (Amersham Biosciences) that was washed with buffer A containing 0.1 M NaCl and eluted with a linear gradient of 0.1–0.5 M NaCl (0.2 ml min^{-1}, total volume 7.5 ml). Fractions with SOX activity were pooled, concentrated in a Centricon YM-30 unit (Millipore, Billerica, MA), loaded on a Superdex 200 HR 10/30 column (Amersham Biosciences) equilibrated in buffer A plus 0.15 M NaCl, and eluted with the same buffer. SOX fractions were identified by SDS-PAGE, pooled, desalted on a 1-ml Sephadex G-25 spin column equilibrated in buffer A plus 10% glycerol, frozen in liquid N_2, and stored at −80 °C. This preparation had no catalase activity, as judged by the 100% recovery of H_2O_2 spikes added to SOX assays. Native molecular mass was estimated using the Superdex 200 HR 10/30 column and thyroglobulin, apoferritin, β-amylase, bovine serum albumin, and carbonic anhydrase as standards. SDS-polyacrylamide gels contained 12.5% polyacrylamide and were stained with Coomassie Blue. Protein was estimated by Bradford's method (26) using bovine serum albumin as the standard.

Proteolysis and Mass Spectrometry—Purified AtSOX (75 μg, in 100 μl of Tris-HCl, pH 8.0, containing 10% glycerol) was mixed with 400 μl of 20 mM Tris-HCl, pH 8.7, and 30 μmol of dithiothreitol and heated at 55 °C for 10 min. Iodoacetamide (20 mg) was then added followed by incubation in darkness at 23 °C for 30 min. The reduced and alkylated protein was precipitated at −20 °C for 18 h with 10 volumes of 10% trichloroacetic acid in acetone containing 0.075% SDS, harvested by centrifugation, washed in cold acetone, and air-dried. The precipitate was dissolved in 200 μl of 50 mM NH_4HCO_3, pH 8.0, and digested with 1 μg of sequencing grade endoproteinase Asp-*N* (Roche Applied Science) at 37 °C for 18 h. Mass spectrometry was carried out in the Protein Chemistry Core Facility at the University of Florida. MALDI-TOF MS analyses used a Voyager DE-Pro instrument (Applied Biosystems, Framingham, MA). Undigested SOX samples were mixed with 0.1% trifluoroacetic acid, adsorbed to a C4 Zip-Tip microcolumn (Millipore), and eluted with 60% acetonitrile containing 0.1% trifluoroacetic acid and 10 mg/ml sinapinic acid. The eluate was spotted onto the sample plate and analyzed in the linear mode. Asp-*N* peptides were treated similarly except that a C18 Zip-Tip was used, α-cyano-4-hydroxycinnamic acid replaced sinapinic acid, and the operation was in the reflectron mode. For peptide analysis, the data evaluated were monoisotopic peaks; mass accuracy was <10 ppm. Precursor and product ion scanning were performed on a Q-Star instrument (Applied Biosystems) equipped with a nanoflow electrospray device and operated in negative ion mode (27).

Identification of Δ^1-Piperideine-6-carboxylate—Purified AtSOX was added to 10 mM L-pipecolate solutions, and the reaction was followed *in situ* by ^{1}H NMR. Spectra (128–1024 transients) were acquired at 500 MHz on a UnityPlus instrument (Varian, Palo Alto, CA) using 90° pulses and a recycle time of 5 s that included the presaturation of the water resonance for 1.9 s. For comparison to Δ^1-piperideine-2-carboxylate, spectra of the product of lysine oxidase acting on lysine were acquired.

Sarcosine Metabolism by Arabidopsis—A 15-day-old plant was washed free of soil, and the lower two-thirds of its root system was severed under water. The plant (0.2 g of fresh weight) was placed with

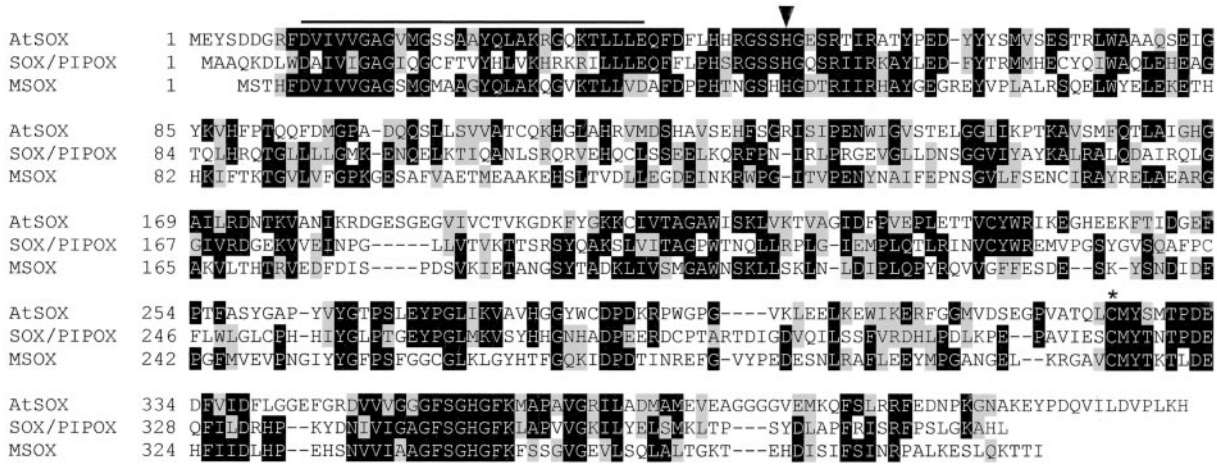

FIG. 1. **Comparison of the *Arabidopsis* SOX homolog to related proteins from other species.** Alignment of the deduced protein sequences of AtSOX, SOX/PIPOX from rabbit (GenBank™ AAB48443), and MSOX from *Bacillus* sp. B-0618 (GenBank™ P40859). Identical residues are *shaded* in *black*, similar residues in *gray*. *Dashes* are gaps introduced to maximize alignment. The *asterisk* marks the cysteine where FAD is covalently attached in *Bacillus* sp. MSOX. The *arrowhead* marks the histidine where FAD is covalently attached in sarcosine and dimethylglycine dehydrogenases. The $\beta\alpha\beta$ ADP-binding fold is *overlined*.

the cut roots in a microcentrifuge tube containing 1.74 μCi (35 nmol) of [carboxyl-^{14}C]sarcosine in 20 μl of water. After incubation for 6 h in the light, adding water to the tube to replace evapotranspiration losses, unabsorbed ^{14}C was quantified, and the plant was ground in liquid N_2 and extracted by gentle agitation in 0.8 ml of 30 mM NH_4HCO_3, pH 8.0, for 20 min at 0 °C. After centrifuging to clear, the extract was mixed with 4 volumes of acetone and recentrifuged. The supernatant was mixed with 8 ml of water and applied to a 1-ml column of AG 50 (H^+) resin. Amino acids were eluted with 5 ml of 2.5 N HCl, lyophilized, and analyzed by thin layer electrophoresis as above. The pellet was washed with 80% acetone, dried, redissolved in 0.75 ml of 6 N HCl, and heated at 110 °C for 12 h. After lyophilizing, the hydrolysate was dissolved in water and analyzed by thin layer electrophoresis. Amino acid zones were located autoradiographically and by reference to standards, and their ^{14}C contents were determined by scintillation counting. [^{14}C]Glycine and [^{14}C]serine data were corrected for label present in these zones in a control sample spiked with [carboxyl-^{14}C]sarcosine before extraction.

Real Time Quantitative RT-PCR—Total RNA was extracted from three samples of each tissue using RNeasy kits (Qiagen, Valencia, CA) and treated with DNase (DNA-*free*™ kit, Ambion, Austin, TX). Real time quantitative RT-PCR was performed on 250 ng of RNA in 25-μl reactions using TaqMan One-Step RT-PCR master mix reagents (Applied Biosystems, Foster City, CA) and an Applied Biosystems GeneAmp 5700 sequence-detection system. The primers and probe (designed with Applied Biosystems Primer Express software) were as follows: forward primer 5′-GGATGGTTGATTCCGAAGGA-3′; reverse primer 5′-TCGTCCGGTGTCATCGAATA-3′; probe 5′-CCGTGGCGACTCAGCTTTGT-3′. The fluorescent reporter dye 6-carboxyfluorescein and the quencher dye 6-carboxytetramethylrhodamine were bonded to the 5′- and 3′-ends, respectively. The amplicon was 64 bp long. RT-PCR conditions were as follows: 48 °C for 30 min and 95 °C for 10 min, followed by 40 cycles of 95 °C for 15 s and 60 °C for 1 min. The standard was sense-strand RNA, prepared as described (28). The template for *in vitro* transcription was PCR-amplified AtSOX cDNA, and the primers were 5′-AATTAACCCTCACTAAAGGGAACAAAAGCTGGCTACGGTGTGTTATTGGAGA-3′ (forward, the T3 promoter sequence is underlined) and 5′-AAAAAAATCACGAAATCCTCGTCC-3′ (reverse). Samples and standards were run in duplicate. A C_T threshold value was determined from amplification curves by selecting an optimal ΔRn (emission of the reporter dye over starting background fluorescence) in the exponential part of the plots.

Preparation of Radiolabeled Proteins for Import into Peroxisomes—Plasmid pMV2 containing a full-length spinach glycolate oxidase cDNA was provided by C. R. Somerville (Carnegie Institution, Stanford, CA). pMV2 was linearized with HindIII and pET43-SOX with XhoI. The linearized DNAs were transcribed using T7 RNA polymerase (Promega). Radiolabeled glycolate oxidase and AtSOX were synthesized in a cell-free rabbit reticulocyte lysate system (Promega) in the presence of [^{35}S]methionine. The efficiency of translation was assessed by trichloroacetic acid precipitation onto glass fiber filters followed by ethanol washes and liquid scintillation counting (29).

Isolation of Pumpkin Glyoxysomes—Glyoxysomes were isolated from pumpkin cotyledons as described previously (29). The glyoxysomal pellet was resuspended in isolation buffer (Hepes-KOH, pH 6.0, 0.3 M mannitol) to a final concentration of 35 mg/ml total protein.

Import Reactions—In vitro protein import reactions (final volume 200 μl) were initiated by adding ^{35}S-labeled glycolate oxidase or AtSOX (5×10^5 cpm trichloroacetic acid-precipitable protein) to 350 μg of glyoxysomes in the presence of import buffer (25 mM Mes-KOH, pH 6.0, 0.5 M sucrose, 10 mM KCl, 1 mM $MgCl_2$, and 5 mM MgATP). The reaction temperature was 26 °C unless otherwise noted. Import reactions were incubated for 30 min and then the glyoxysomes were treated with thermolysin (25 μg/ml in 0.5 mM $CaCl_2$) to remove non-imported proteins. Protease treatment was for 30 min on ice; reactions were stopped by adding EDTA (10 mM final concentration) to inhibit the thermolysin. The protease-treated glyoxysomes were then repurified on a sucrose cushion, solubilized in SDS sample buffer, and subjected to SDS-PAGE as described (29). Note that only proteins protected by an intact glyoxysomal membrane would be protease-resistant. Lysed or compromised organelles would not be recovered from the sucrose cushion. Where indicated, samples were treated with Triton X-100 (1% v/v final concentration) to lyse the organelles following import and protease treatment as described (29).

Amino Acid Analysis—Samples (0.4–1.2 g fresh weight, 10–30 plants) were frozen in liquid N_2 and stored at −20 °C. Extraction was for 48 h at 4 °C with 10 ml of methanol containing 250 nmol of 3,4-dehydro-DL-proline as an internal standard, followed by phase separation by adding $CHCl_3$ (5 ml) and water (6 ml); the aqueous phase was dried in an air stream, redissolved in 1 ml of water, and applied to 1 × 4.5-cm columns of AG 50 (H^+). After washing columns with 8 ml of water, amino acids were eluted with 6 ml of 6 M NH_4OH and dried. Amino acids were then derivatized with 200 μl of isobutyl alcohol:acetyl chloride (5:1 v/v) (120 °C, 20 min), dried, then derivatized with 100 μl of heptafluorobutyric anhydride (120 °C, 10 min). Samples were brought to near dryness and redissolved in 100 μl of ethyl acetate:acetic anhydride 1:1 (v/v), of which 1-μl aliquots were analyzed by GC and electron ionization GC-MS, essentially as described (30). Response factors were determined using an amino acid standard mixture (Sigma) supplemented with 250 nmol of 3,4-dehydro-DL-proline, sarcosine, α-amino-*n*-butyrate, or DL-pipecolic acid. Tests showed that sarcosine and pipecolic acid added to *Arabidopsis* extracts were recovered quantitatively after processing as described above.

RESULTS

Characterization of a SOX cDNA from Arabidopsis—Searches of GenBank™ revealed a single intronless *Arabidopsis* gene (*At2g24580*) encoding a putative SOX protein and five cognate *Arabidopsis* ESTs. Sequencing of a full-length EST confirmed that it specifies a protein (AtSOX) with ~33% overall sequence identity to mammalian SOX/PIPOX and *Bacillus* MSOX (Fig. 1). The AtSOX sequence has the features charac-

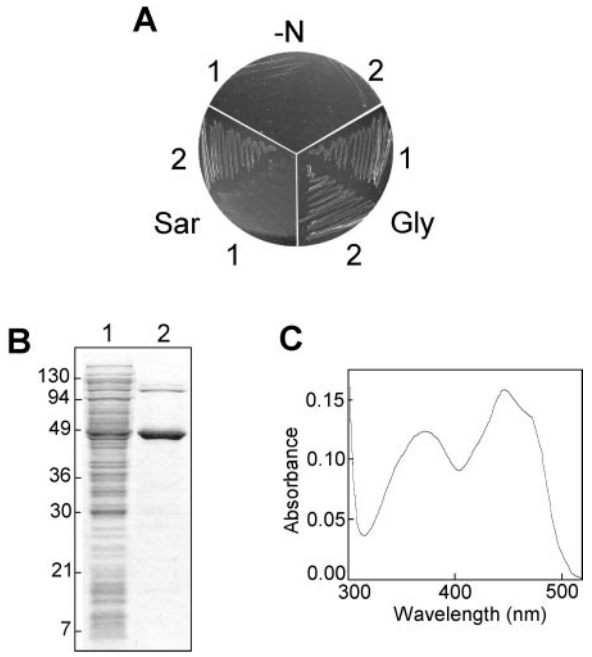

FIG. 2. **Recombinant AtSOX expression, purification, and absorption spectrum.** *A*, functional expression of AtSOX in *E. coli* Rosetta™ (DE3) cells harboring pET-43.1a alone (*1*) or containing the AtSOX cDNA (*2*) were grown at 25 °C for 4 days on minimal medium plates without any nitrogen source (−*N*), or with glycine (*Gly*) or sarcosine (*Sar*) as a nitrogen source. *B*, SDS-polyacrylamide gel electrophoresis of soluble proteins of Rosetta™ (DE3) cells after induction of AtSOX expression by isopropyl-D-thiogalactopyranoside (*lane 1*), and the AtSOX protein after $(NH_4)_2SO_4$, MonoQ, and Superdex 200 steps (*lane 2*). Staining was done with Coomassie Blue. Positions of molecular markers (kDa) are marked. *C*, absorption spectrum of purified AtSOX (0.8 mg/ml) in 50 mM Tris-HCl, pH 8.0.

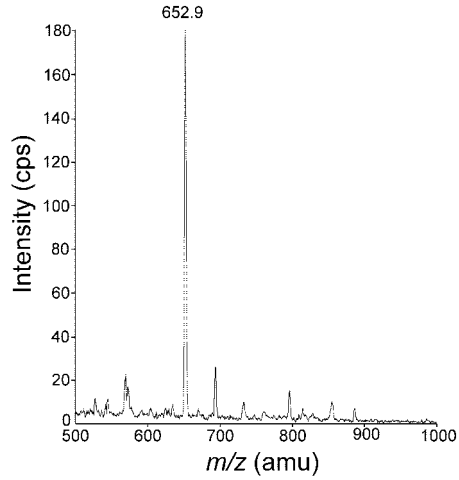

FIG. 3. **Electrospray mass spectrum of the FAD-containing peptide from an Asp-*N* digest of AtSOX.** Phosphate-containing fragments were detected using precursor ion scanning in the negative ion mode. The peak at 652.9 mass units corresponds to the quadruply charged ion of the flavinated peptide Asp^{315}-Pro^{331}. The mass range analyzed was 500–1400 atomic mass units; no signals >1000 atomic mass units were detected. Minor spectral peaks may correspond to traces of phosphopeptides in the digest.

teristic of the MSOX family (5, 7) including a $\beta\alpha\beta$-fold (31) near the N terminus and a conserved cysteine residue (Cys^{325}) in the C-terminal region that, in MSOX, is the covalent attachment site of FAD (8) (Fig. 1). There is also a conserved histidine near the N terminus (His^{50}) that aligns with the covalent attachment site of FAD in sarcosine and dimethylglycine dehydrogenases (8, 32). However, a difference from mammalian SOX/PIPOX is that the C-terminal tripeptide, LKH, is not a classical PTS1 signal (5, 33). Further data base searches using the AtSOX protein as the query detected a rice gene (*B1012D10.21*) and ~130 ESTs from a range of dicots and monocots encoding close homologs of AtSOX, showing that SOX-like proteins are widespread among angiosperms. Phylogenetic comparisons between the AtSOX and rice SOX sequences and other members of the MSOX family indicated that the plant proteins cluster with mammalian SOX/PIPOXs (data not shown).

Use of Sarcosine As Sole Nitrogen Source by E. coli Expressing AtSOX—Wild type *E. coli* uses glycine as the sole nitrogen source (34) but is not expected to use sarcosine as efficiently because of low endogenous SOX activity (35). Consistent with this prediction, growth of wild type cells on plates was poor when sarcosine replaced glycine as the nitrogen source (Fig. 2*A*). However, when the cells carried an AtSOX expression plasmid, growth on sarcosine was comparable with growth on glycine (Fig. 2*A*). This functional expression result indicates that AtSOX has SOX activity *in vivo*.

Characterization of the AtSOX Protein—Recombinant AtSOX extracted from *E. coli* cells was purified 7-fold with an overall yield of 1.7% by $(NH_4)_2SO_4$ fractionation, anion exchange, and size exclusion chromatography. The purified protein was 90% homogeneous as assessed by the densitometry of the gel shown in Fig. 2*B*, was catalase-free, and showed high activity with sarcosine as a substrate. Its k_c value (0.91 s^{-1} at 30 °C) was midway between those of mammalian SOX/PIPOX and *Bacillus* MSOX, being about 10-fold above the former and 10-fold below the latter (5, 8, 36). The molecular mass estimated from denaturing gel electrophoresis (Fig. 2*B*, 46 kDa) was the same as for SOX/PIPOX and MSOX, which are 44–46-kDa proteins (5, 8, 36). Size exclusion chromatography indicated that AtSOX has a molecular mass of 60 kDa (data not shown), indicating that, like MSOX, it is active as a monomer. Purified SOX was yellow and had a typical flavoprotein absorbance spectrum with peaks at 373 and 452 nm and a shoulder at 475 nm (Fig. 2*C*). After precipitation with 5% trichloroacetic acid, all of the chromophore was associated with the pellet and reentered solution when the pellet was dissolved in 5 M guanidine HCl. This behavior indicates that the flavin is covalently bound to the enzyme, as in other members of the MSOX family (5, 7). The flavin content was 0.97 mol/mol of protein, estimated as described (8) from the absorbance spectrum of the guanidine-denatured enzyme, assuming that the contaminant proteins (10% of the total in the preparation) were not flavinated. Consistent with there being one covalently bound flavin/mol, the molecular mass of AtSOX estimated by MALDI-TOF MS was 46,475 ± 13 Da (mean ± S.E., $n = 4$), which matches the predicted value (46,485.6 Da) for the apoprotein (45,702 Da) plus a FAD residue (783.6 Da). The mass spectral data showed no peak corresponding to the apoenzyme. AtSOX enzyme activity was not stimulated by FAD addition.

Localization of the Covalent Flavin Attachment Site—To determine whether Cys^{325} or, less probably, His^{50} is the FAD attachment site, the reduced AtSOX protein was alkylated with iodoacetamide and then cleaved with Asp-*N* protease. The digest was analyzed by MALDI-TOF MS, focusing particularly on the peptides Asp^{41}-Glu^{62} and Asp^{315}-Pro^{331}. The sequence coverage was 81.7% and included the Asp^{41}-Glu^{62} fragment, for which a peptide with the mass ($[M+H]^+$) calculated for the unflavinated form (2553) was found (data not shown). This indicates that the flavin is not bound to His^{50}. No flavinated peptides were seen in the MALDI-TOF spectrum, which was not unexpected as such peptides are not easily ionized. Precursor ion scanning was therefore used to detect flavinated peptides by searching for precursors of the phosphate fragment ion (PO_3^-, −79 atomic mass units) in negative ion mode (27). A

TABLE I
Relative activity of AtSOX toward various subtrates

Assays (20 μl) contained 0.25 μg of purified AtSOX protein and 10 mM amino acid. For carbinolamines, which form spontaneously in mixtures of amino acid and formaldehyde (37), 10 mM formaldehyde was also added. Assays were incubated for 60 or 120 min. H_2O_2 formation was quantified colorimetrically. Data are expressed relative to the activity with sarcosine as substrate (208-310 nmol min^{-1} mg^{-1} protein) and are based on three replicates.

Substrate	Relative activity
	%
Sarcosine	100
N-Methyl-L-alanine	124
N-Methyl-L-leucine	210
N-Methyl-D,L-valine	136
L-Pipecolate	275
D-Pipecolate	<2[a]
L-Proline	8.9
D-Proline	40
N-Methyl-L-tryptophan	<2
Dimethylglycine	<2
Carbinolamines	
L-Methionine + Formaldehyde	9.3[b]
Glycine + Formaldehyde	<2
L-Lysine + Formaldehyde	<2
L-Tryptophan + Formaldehyde	<2

[a] Detection limit was 2% of the activity with sarcosine.
[b] No activity was observed with either L-methionine or formaldehyde alone.

phosphate-containing peptide was detected at *m/z* 652.9 (Fig. 3), as predicted for the quadruply charged flavinated Asp^{315}-Pro^{331} peptide (expected mass 2612). This result was supported by finding the phosphate product of the triply charged ion by product ion scanning (data not shown). These results unambiguously identify Cys^{325} as the attachment site, because, were the FAD attached elsewhere (*e.g.* to Tyr^{327}), Cys^{325} would have been alkylated, resulting in a flavopeptide of mass 2669.

Substrates and Products of AtSOX—Tests with compounds that are substrates for various members of the MSOX family showed that AtSOX had high activity with other *N*-methyl amino acids and L-pipecolate and low activity with L-proline (Table I). The D-enantiomer of proline, but not pipecolate, was also attacked, as was the *N*-hydroxymethyl (carbinolamine) derivative of L-methionine (Table I). Carbinolamines are also substrates of *N*-methyltryptophan oxidase (37). The K_m values for sarcosine, L-pipecolate, and *N*-methyl-L-leucine were 4.22, 5.18, and 0.66 mM, and the k_c values were 0.91, 2.91, and 0.62 s^{-1}. Thus, by the criterion of catalytic efficiency (k_c/K_m), *N*-methyl-L-leucine was the best of these three substrates, although not strongly preferred over the others. As in the case of bacterial MSOX (38), adding 50 μM (6*R*,6*S*)-tetrahydrofolate did not increase reaction rates, indicating that tetrahydrofolate is not a substrate for AtSOX.

With sarcosine as a substrate, the products were H_2O_2, glycine, and formaldehyde in a stoichiometry of 1:1.03 ± 0.03: 0.98 ± 0.04 (mean ± S.E., $n = 3$). This finding rules out an alternative possibility, namely that the reaction forms H_2O_2, glyoxylate, and methylamine, as occurs when sarcosine is oxidized by glycine oxidase (11). To determine whether oxidation of L-pipecolate gave Δ^1-piperideine-6-carboxylate (P6C) or, less probably, Δ^1-piperideine-2-carboxylate (P2C), the reaction product was derivatized with 2-aminobenzaldehyde. The adduct showed an absorption maximum at 465 nm, which is diagnostic for P6C, the P2C adduct having a maximum at 450 nm (39). ^1H NMR analysis also indicated that the reaction yields P6C. The course of the reaction was followed by acquiring successive spectra of reactions containing SOX and L-pipecolate, because the rate of P6C synthesis *in vitro* was comparable with the rate of its spontaneous degradation. During the reaction, resonances were observed close to 1.4, 1.7, 2.0, and 3.8 ppm, which are characteristic of P6C (40), and their intensities were consistent with the extent of reaction determined from the absorbance of the 2-aminobenzaldehyde adduct. Comparison with NMR spectra of lysine oxidase reaction mixtures containing P2C, which is stable, showed that SOX does not make P2C from L-pipecolate.

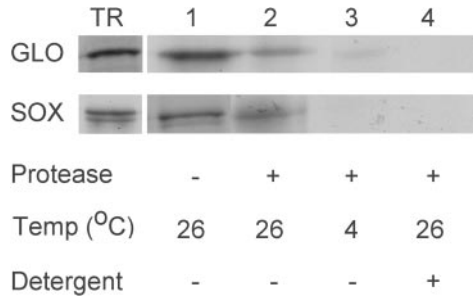

FIG. 4. ***In vitro* import of spinach glycolate oxidase and AtSOX into pumpkin glyoxysomes.** Isolated glyoxysomes were incubated with radiolabeled glycolate oxidase (*GLO*, *top*) or AtSOX (*SOX*, *bottom*) under standard import conditions (see under "Experimental Procedures") at either 26 °C (*lanes 1, 2,* and *4*) or 4 °C (*lane 3*). After import, samples in *lanes 2–4* were treated with the protease thermolysin. The detergent Triton X-100 was added to the sample in *lane 4* to lyse the organelles. The results shown are from representative experiments that were repeated three times. *TR*, translation products, ~10% of the amount of protein presented to glyoxysomes for import.

In Vitro Import of AtSOX into Peroxisomes—Although AtSOX has neither an orthodox PTS1 tripeptide at the C terminus nor a PTS2 signal (41) near the N terminus, the peroxisomal location of mammalian SOX/PIPOXs prompted us to test for the peroxisomal import of AtSOX. We used an *in vitro* assay based on pumpkin glyoxysomes, a type of peroxisome found in cotyledons of oilseed plants, and included the leaf peroxisomal enzyme glycolate oxidase as a positive control (29). After incubation with glyoxysomes at 26 °C, both AtSOX and glycolate oxidase became protease-resistant, indicating protection by the organelle membrane (Fig. 4, *lanes 1* and *2*); consistent with this, the protection was lost when a detergent was added (Fig. 4, *lane 4*). No import was seen at 4 °C (*lane 3*), which is characteristic of the peroxisomal transport process (29). These results demonstrate that AtSOX is imported into the peroxisomes, despite the absence of a typical targeting sequence. We were not able to establish this point by the more direct approach of subcellular fractionation of *Arabidopsis* tissues, because SOX activity in tissue extracts was too low to quantify.

Expression of AtSOX in Arabidopsis Organs—The expression of the AtSOX gene was analyzed by real time quantitative RT-PCR rather than RNA blotting because EST data indicate that this gene is not highly expressed (only five of ~1.8×10^5 *Arabidopsis* ESTs in the EST data base are AtSOX sequences). AtSOX mRNA was detected in wild type plants in all of the organs tested, at levels ranging from 35 to 82 fg/250 ng of total RNA (Table II). This corresponds to an mRNA frequency no higher than 1 in 30,000 assuming mRNA to be ~1% of total RNA. AtSOX is thus expressed at low levels throughout the plant. Because bacterial MSOX is induced by sarcosine (3) we tested the effect of applying 10 mM sarcosine as a foliar spray, which is an effective way to obtain sarcosine entry (17). This treatment did not change the AtSOX mRNA level in leaves (Table II).

Metabolism of Sarcosine—To verify that *Arabidopsis* can metabolize sarcosine to glycine *in vivo*, we supplied [carboxyl-^{14}C]sarcosine to the shoot via the transpiration stream and analyzed the labeling of free and protein-bound amino acids. After 6 h, 1.66 μCi (33.3 nmol) of [^{14}C]sarcosine had been absorbed (95% of that supplied), and most of this (1.40 μCi,

TABLE II
AtSOX mRNA levels in wild type Arabidopsis and RNAi transgenics and the effect of sarcosine

The RNAi transgenics were T2 generation plants. Levels of mRNA were determined by real time quantitative RT-PCR. Sarcosine (10 mM) was applied as a foliar spray 24 h before harvest. Three independent RNA extracts were made of each organ, and duplicate mRNA determinations were made on each extract. Data are means of all six determinations ± S.E. An internal AtSOX RNA standard was added to each sample to enable correction for recovery from RT-PCR.

Genotype	Organ	AtSOX mRNA
		fg/250 ng total RNA
Wild type	Young leaves	50 ± 9
	Mature leaves	50 ± 11
	Mature leaves + sarcosine	35 ± 8
	Stems	40 ± 11
	Roots	63 ± 16
	Siliques	82 ± 22
RNAi progeny S14	Mature leaves	5.4 ± 0.6
RNAi progeny S16	Mature leaves	4.2 ± 0.2
RNAi progeny S17	Mature leaves	8.3 ± 0.8

28.0 nmol) was recovered as free sarcosine. As the shoot fresh weight was 0.2 g, this corresponds to a sarcosine metabolism rate of 4.4 nmol g^{-1} h^{-1}. No ^{14}C was detected in free pools of glycine or its metabolite serine, but the protein-bound glycine and serine pools were significantly labeled (3.0 and 1.3 nCi, respectively). (In experiments of this type more label is expected to accumulate in protein-bound than free pools because of their larger size and slower turnover.) No other labeled amino acids were detected, indicating that ^{14}C reached glycine and serine directly by the path sarcosine → glycine → serine and not indirectly via $^{14}CO_2$. These results show that sarcosine can be converted to glycine by *Arabidopsis* shoots but at a very low rate relative to other fluxes in glycine metabolism. Assuming that sarcosine is metabolized solely via glycine, the rate of glycine formation by this route (4.4 nmol g^{-1} h^{-1}) would be only ~0.1% of the rate of glycine production by photorespiration in leaves (42).

Silencing of AtSOX Expression by RNAi—To assess the physiological significance of AtSOX, we transformed *Arabidopsis* with an RNAi construct in the pHELLSGATE vector (22). Individuals harboring the construct were identified among the segregating progenies of transformed plants by their kanamycin resistance and then grown in soil to the rosette stage and pooled for analysis. Measurement of the AtSOX mRNA level by real time quantitative RT-PCR identified three progenies showing a high degree (83–92%) of silencing (Table II). These RNAi plants exhibited no obvious differences in vegetative or reproductive growth from wild type plants (not shown).

Amino Acid Levels in Wild Type and AtSOX-RNAi Transgenic Arabidopsis—The free amino acid pools of wild type and RNAi plants were analyzed by GC-MS, with special focus on sarcosine, pipecolate, and related metabolites. In wild type plants, sarcosine was barely detectable (0.6 nmol g^{-1} of fresh weight) in rosette leaves (Table III) and was no more abundant in flowering shoots or roots (data not shown). There was no accumulation of sarcosine in RNAi plants (Table III). In contrast, pipecolate was readily detectable in wild type rosettes (10 nmol g^{-1} of fresh weight) and accumulated 6-fold in RNAi plants (Table III). Moreover, the pipecolate metabolite α-aminoadipate was 30-fold less abundant in RNAi plants (Table III). Glycine and lysine levels did not differ significantly between wild type and RNAi plants (Table III). Nor were there marked differences in other amino acids, although there were small decreases (30–50%) in serine, valine, leucine, isoleucine, and histidine pools in RNAi plants (not shown).

TABLE III
Levels of free amino acids in rosette leaves of wild type Arabidopsis and AtSOX-RNAi transgenics

Rosette leaves of vegetative plants were harvested after 22 days growth. Amino acids were quantified by GC-MS of *N*(*O*,*S*)-heptafluorobutyryl isobutyl derivatives. Data are means ± S.E. for RNAi progenies S14, S16, and S17 or for four replicate samples of wild type plants.

Amino acid	Wild type	RNAi transgenics
	nmol g^{-1} of fresh weight	
Sarcosine	0.6 ± 0.1	0.6 ± 0.05
Pipecolate	10 ± 2	62 ± 15[a]
α-Aminoadipate	15 ± 4	0.5 ± 0.28[b]
Glycine	140 ± 26	118 ± 3
Lysine	35 ± 9	20 ± 3

[a] $p < 0.01$ (by Student's t test).
[b] $p < 0.05$.

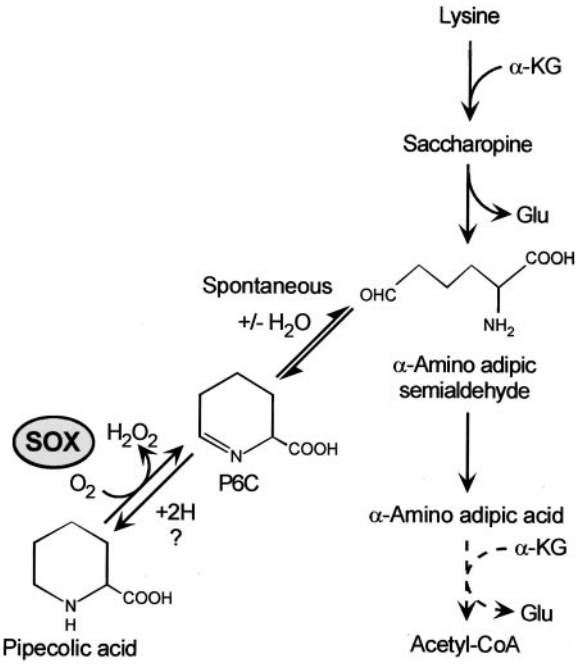

FIG. 5. **Scheme showing the relationship between lysine catabolism and pipecolate.** The vertical series of reactions is the α-amino adipic acid pathway of lysine catabolism, of which pipecolic acid formation is a side branch. *α-KG*, α-ketoglutarate.

DISCUSSION

Our results establish that *Arabidopsis* AtSOX belongs to the eukaryotic branch of the MSOX family and suggest that such enzymes occur in all higher plants. Like its close homologs in other organisms, AtSOX catalyzes the oxidation of sarcosine, other *N*-methyl amino acids, and L-pipecolate, producing formaldehyde and glycine from sarcosine and P6C from pipecolate. Consistent with this catalytic conformity, AtSOX is very like its counterparts in structure, being a ~46-kDa monomer with a covalently attached FAD molecule. As in bacterial MSOX and *N*-methyltryptophan oxidase (7, 8), the FAD of AtSOX is linked to a conserved cysteine residue near the C terminus. The FAD linkage site has not previously been determined for a eukaryotic SOX enzyme.

Because AtSOX was expected, like mammalian SOX/PIPOX, to be a peroxisomal enzyme it was interesting to find that its C-terminal tripeptide (LKH) deviates widely from the standard consensus PTS1 motif (SKL or similar sequences). However, AtSOX was efficiently targeted to peroxisomes *in vitro* implying that its C terminus is indeed a functional PTS1 despite its deviance. This finding adds to the growing evidence that plant PTS1s vary far more than those in animals (33, 43). Because we

found that most SOX proteins specified by ESTs or genomic sequences from other plants also lack classical PTS1s, SOX proteins may be valuable in future studies of peroxisome biogenesis.

That AtSOX is expressed at a low level throughout the plant and is not sarcosine-induced suggests a housekeeping role for this enzyme. We propose that this role is pipecolate oxidation, based on the accumulation of pipecolate and the depletion of α-aminoadipate when AtSOX expression is suppressed. Pipecolate formation in plants is a side-branch of lysine catabolism via the α-amino adipic acid pathway (44, 45) (Fig. 5). One of the intermediates in this pathway, α-amino adipic semialdehyde, spontaneously cyclizes to P6C (46), which upon reduction yields pipecolate (Fig. 5). The enzymatic basis of this reduction is not known in plants, but in *E. coli* it is mediated by the proline biosynthetic enzyme Δ^1-pyrroline-5-carboxylate reductase (47). Because the equilibrium for the reduction step presumably lies far in favor of pipecolate (by analogy with Δ^1-pyrroline-5-carboxylate reduction, see Ref. 48), an essentially irreversible flux from lysine to pipecolate seems likely, especially as saccharopine dehydrogenase (the enzyme that forms α-amino adipic semialdehyde) and Δ^1-pyrroline-5-carboxylate reductase are both cytosolic (44, 49). In this scenario, SOX serves as a salvage enzyme recycling pipecolate back to P6C and thence to α-amino adipic semialdehyde and the rest of the lysine catabolic pathway (Fig. 5), thereby preventing pipecolate accumulation. The very large reduction (30-fold) in α-aminoadipate associated with AtSOX suppression suggests that most of the flux in lysine catabolism in suppressed plants is diverted into pipecolate, which has become a dead end.

Although *Arabidopsis* seems not to produce sarcosine, exogenously supplied sarcosine was slowly metabolized to glycine indicating that sarcosine present in the environment can be utilized. Moreover, AtSOX expression in *E. coli* enhanced sarcosine utilization. We therefore suggest that sarcosine oxidation is a secondary role of AtSOX and plant SOXs in general. The ability to exploit sarcosine opportunistically may be ecologically significant, because sarcosine, derived from creatinine in animal urine, is a common soil metabolite (3). A parallel may be drawn between sarcosine and urea, which is also excreted in large amounts by animals and is absorbed and metabolized by plants (50). The ability of SOX to attack various *N*-methyl amino acids other than sarcosine may also be ecologically significant. *N*-Methyl amino acids are quite widely distributed in nature (12) and as structural analogs of protein amino acids are potential antimetabolites (51). SOX could serve to detoxify them.

Acknowledgments—We thank Emily A. Davis and Anthony G. Visioni for technical assistance with *in vitro* import experiments and Drs. Nancy Denslow and Stanley Stevens of the University of Florida Protein Chemistry Core Facility for mass spectral analyses of SOX.

REFERENCES

1. Balaghi, M., Horne, D. W., and Wagner, C. (1993) *Biochem. J.* **291,** 145–149
2. Yeo, E. J., Briggs, W. T., and Wagner, C. (1999) *J. Biol. Chem.* **274,** 37559–37564
3. Kvalnes-Krick, K., and Jorns, M. S. (1991) in *Chemistry and Biochemistry of Flavoenzymes* (Muller, F., ed) pp. 425–435, CRC Press, Boca Raton, FL
4. Wyss, M., and Kaddurah-Daouk, R. (2000) *Physiol. Rev.* **80,** 1107–1213
5. Reuber, B. E., Karl, C., Reimann, S. A., Mihalik, S. J., and Dodt, G. (1997) *J. Biol. Chem.* **272,** 6766–6776
6. Chikayama, M., Ohsumi, M., and Yokota, S. (2000) *Histochem. Cell Biol.* **113,** 489–495
7. Trickey, P., Wagner, M. A., Jorns, M. S., and Mathews, F. S. (1999) *Structure* **7,** 331–345
8. Wagner, M. A., Khanna, P., and Jorns, M. S. (1999) *Biochemistry* **38,** 5588–5595
9. Wagner, M. A., and Jorns, M. S. (2000) *Biochemistry* **39,** 8825–8829
10. Venci, D., Zhao, G., and Jorns, M. S. (2002) *Biochemistry* **41,** 15795–15802
11. Job, V., Marcone, G. L., Pilone, M. S., and Pollegioni, L. (2002) *J. Biol. Chem.* **277,** 6985–6993
12. Hunt, S. (1985) in *Chemistry and Biochemistry of the Amino Acids* (Barrett, G. C., ed) pp. 55–138, Chapman and Hall, London
13. Rontein, D., Basset, G., and Hanson, A. D. (2002) *Metab. Eng.* **4,** 49–56
14. Farrés, J., Holmberg, N., Schlattner, U., Bailey, J. E., Wallimann, T., and Kallio, P. T. (2002) *Transgenic Res.* **11,** 49–59
15. Hanson, A. D., Gage, D. A., and Shachar-Hill, Y. (2000) *Trends Plant Sci.* **5,** 206–213
16. Hanson, A. D., and Roje, S. (2001) *Annu. Rev. Plant Physiol. Plant Mol. Biol.* **52,** 119–137
17. Hourton-Cabassa, C., Ambard-Bretteville, F., Moreau, F., Davy de Virville, J., Rémy, R., and Francs-Small, C. C. (1998) *Plant Physiol.* **116,** 627–635
18. Olson, B. J., Skavdahl, M., Ramberg, H., Osterman, J. C., and Markwell, J. (2000) *Plant Sci.* **159,** 205–212
19. Li, R., Bonham-Smith, P. C., and King, J. (2001) *Can. J. Bot.* **79,** 796–804
20. Galili, G., Tang, G., Zhu, X., and Gakière, B. (2001) *Curr. Opin. Plant Biol.* **4,** 261–266
21. Gibeaut, D. M., Hulett, J., Cramer, G. R., and Seemann, J. R. (1997) *Plant Physiol.* **115,** 317–319
22. Wesley, S. V., Helliwell, C. A., Smith, N. A., Wang, M. B., Rouse, D. T., Liu, Q., Gooding, P. S., Singh, S. P., Abbott, D., Stoutjesdijk, P. A., Robinson, S. P., Gleave, A. P., Green, A. G., and Waterhouse, P. M. (2001) *Plant J.* **27,** 581–590
23. Bechtold, N., Ellis, J., and Pelletier, G. (1993) *C. R. Acad. Sci.* (*Paris*) **316,** 1194–1199
24. Sambrook, J., Fritsch, E. F., and Maniatis, T. (1989) *Molecular Cloning: A Laboratory Manual*, Cold Spring Harbor Laboratory, Cold Spring Harbor, NY
25. Neidhardt, F. C., Bloch, P. L., and Smith, D. F. (1974) *J. Bacteriol.* **119,** 736–747
26. Bradford, M. M. (1976) *Anal. Biochem.* **72,** 248–254
27. Newton-Vinson, P., Hubalek, F., and Edmondson, D. E. (2000) *Protein Expression Purif.* **20,** 334–345
28. Rontein, D., Wu, W. I., Voelker, D. R., and Hanson, A. D. (2003) *Plant Physiol.* **132,** 1678–1687
29. Brickner, D. G., Harada, J. J., and Olsen, L. J. (1997) *Plant Physiol.* **113,** 1213–1221
30. Rhodes, D., Handa, S., and Bressan, R. A. (1986) *Plant Physiol.* **82,** 890–903
31. Wierenga, R. K., Terpstra, P., and Hol, W. G. (1986) *J. Mol. Biol.* **187,** 101–107
32. Mewies, M., McIntire, W. S., and Scrutton, N. S. (1998) *Protein Sci.* **7,** 7–20
33. Olsen, L. J. (1998) *Plant Mol. Biol.* **38,** 163–189
34. Reitzer, L. J. (1996) in *Escherichia coli and Salmonella-Cellular and Molecular Biology* (Neidhardt, F. C., ed) pp. 380–390, ASM Press, Washington D. C.
35. Khanna, P., and Jorns, M. S. (2001) *Biochemistry* **40,** 1441–1450
36. Mihalik, S. J., McGuinness, M., and Watkins, P. A. (1991) *J. Biol. Chem.* **266,** 4822–4830
37. Khanna, P., and Jorns, M. S. (2001) *Biochemistry* **40,** 1451–1459
38. Wagner, M. A., and Jorns, M. S. (1997) *Arch. Biochem. Biophys.* **342,** 176–181
39. Soda, K., Misono, H., and Yamamoto, T. (1968) *Biochemistry* **11,** 4102–4109
40. Rumbero, A., Martin, J. F., Lumbreras, M. A., Liras, P., and Esmahan, C. (1995) *Bioorg. Med. Chem.* **3,** 1237–1240
41. Johnson, T. L., and Olsen, L. J. (2001) *Plant Physiol.* **127,** 731–739
42. Rébeillé, F., and Douce, R. (1999) in *Regulation of Primary Metabolic Pathways in Plants* (Kruger, N. J., Hill, S. A., and Ratcliffe, R. G., eds) pp. 53–99, Kluwer, Dordrecht
43. Mullen, R. T., Lee, M. S., Flynn, C. R., and Trelease, R. N. (1997) *Plant Physiol.* **115,** 881–889
44. Arruda, P., Kemper, E. L., Papes, F., and Leite, A. (2000) *Trends Plant Sci.* **5,** 324–330
45. Galili, G. (2002) *Annu. Rev. Plant Physiol. Plant Mol. Biol.* **53,** 27–43
46. Aspen, A. J., and Meister, A. (1962) *Biochemistry* **1,** 600–605
47. Fujii, T., Mukaihara, M., Agematu, H., and Tsunekawa, H. (2002) *Biosci. Biotechnol. Biochem.* **66,** 622–627
48. Pahlich, E., Jäger, H.-J., and Kaschel, E. (1981) *Z. Pflanzenphysiol.* **101,** 137–144
49. Verbruggen, N., Villarroel, R., and Van Montagu, M. (1993) *Plant Physiol.* **103,** 771–781
50. Liu, L. H., Ludewig, U., Frommer, W. B., and Von Wiren, N. (2003) *Plant Cell* **15,** 790–800
51. Harborne, J. B. (1993) *Introduction to Ecological Biochemistry*, pp. 73–74, Academic Press, San Diego, CA